Published in final edited form as:
Prostaglandins Leukot Essent Fatty Acids. 2011 July ; 85(1): 43–52. doi:10.1016/j.plefa.2011.04.022.

Inhibition of 5-lipoxygenase activity in mice during cuprizone-induced demyelination attenuates neuroinflammation, motor dysfunction and axonal damage

K. Yoshikawa[†], **S. Palumbo**, **C. D. Toscano**, and **F. Bosetti**[§,*]
Molecular Neuroscience Unit, Brain Physiology and Metabolism Section, National Institute on Aging, National Institute of Health, Bethesda, MD, USA

Abstract

Multiple sclerosis (MS) is a chronic, inflammatory demyelinating disease of the central nervous system (CNS). Increased expression of 5-lipoxygenase (5-LO), a key enzyme in the biosynthesis of leukotrienes (LTs), has been reported in MS lesions and LT levels are elevated in the cerebrospinal fluid of MS patients. To determine whether pharmacological inhibition of 5-LO attenuates demyelination, MK886, a 5-LO inhibitor, was given to mice fed with cuprizone. Gene and protein expression of 5-LO were increased at the peak of cuprizone-induced demyelination. Although MK886 did not attenuate cuprizone-induced demyelination in the corpus callosum or in the cortex, it attenuated cuprizone-induced axonal damage and motor deficits and reduced microglial activation and IL-6 production. These data suggest that during cuprizone-induced demyelination, the 5-LO pathway contributes to microglial activation and neuroinflammation and to axonal damage resulting in motor dysfunction. Thus, 5-LO inhibition may be a useful therapeutic treatment in demyelinating diseases of the CNS.

1. Introduction

Multiple sclerosis (MS) is a chronic inflammatory demyelinating disease of the central nervous system (CNS) characterized by recurrent and progressive demyelination/remyelination cycles, resulting in development of scleroses in both the white and gray matter of the CNS [1], axonal damage, neuroinflammation, and neuronal loss [2,3]. Demyelination is accompanied by depletion of oligodendrocyte precursor cells, loss of mature oligodendrocytes, astrogliosis, and infiltration of macrophages/microglia and T lymphocytes [4].

The cuprizone model of demyelination [5] is charachterized by apoptotic death of mature oligodendrocytes [6,7], and is accompanied by neuroinflammation [8] and motor dysfunction [9]. Four patterns have been described in MS lesions, with patterns I and II

[§]Corresponding author: Francesca Bosetti, Pharm.D., Ph.D., 9 Memorial Drive, Rm. 1S126 MSC 0947, Bethesda MD 20892-0947, Phone: (301) 594-5077, Fax: (301) 402-0074, frances@mail.nih.gov.
[†]Present address: Department of Pharmacology, Faculty of Medicine, Saitama Medical University, 38 Morohongo Moroyama-machi, Iruma-gun, Saitama, Japan 350–0495
[*]Present address: National Institute of Neurological Disorders and Stroke, NIH, Neuroscience Center, Room 2118; 6001 Executive Blvd., Bethesda, MD 20892

Competing Interests: The authors declare that they have no competing interests.

showing similarities to T-cell-mediated or T-cell plus antibody-mediated autoimmune encephalomyelitis, respectively, and patterns III and IV lesions suggesting a primary oligodendrocyte damage and degeneration, reminiscent of virus- or toxin-induced demyelination rather than autoimmunity [10]. Thus, the cuprizone model of demyelination is closer to patterns III and IV lesions in reproducing a primary demyelination that is independent from the immune system, and axonal damage. Mice show progressive demyelination when they are kept on a 0.2% cuprizone diet, with a peak in demyelination observed after 5 weeks of cuprizone [6,11]. Cuprizone withdrawal from the diet results in a remyelination after several weeks [12].

Omega-6 fatty acids, such as linoleic acid, γ-linoleic acid and arachidonic acid, have been implicated in demyelinating disease. Linoleic acid and γ-linoleic acid have shown protective effects in MS and experimental autoimmune encephalomyelitis (EAE) [13–16]. On the other hand, arachidonic acid cascade is suggested to become activated during demyelination[17,18]. Increased expression of 5-lipoxygenase (5-LO) in lesions [19,20] and of 5-LO-derived leukotriene (LT) products in the cerebrospinal fluid [21] has been reported in patients with MS. 5-LO, a key enzyme in the biosynthesis of LTs [22] is activated by 5-LO-activating protein (FLAP) and converts arachidonic acid to LTA_4, which is then converted to LTB_4 by LTA_4 hydrolase [23,24], or to a cysteinyl-LT (such as LTC_4, LTD_4 or LTE_4) by LTC_4 synthase [25,26].

MK886 is a 5-LO inhibitor that binds to FLAP and thereby prevents 5-LO activation [27]. *In vitro*, MK886 inhibits LTs biosynthesis in leukocytes [28]. *In vivo*, systemic administration of MK886 has been shown to inhibit LPS-induced hypothalamic LT production [29] and cortical cysteinyl-LT production induced by permanent occlusion of the middle cerebral artery [30].

In this study, to determine whether 5-LO activity contributes to the pathological events associated with demyelination and associated neuroinflammation, we administered MK886 to cuprizone-exposed mice. We demonstrated that, although MK886 did not attenuate cuprizone-induced demyelination in the corpus callosum and cortex, it reduced microglial activation, IL-6 production, axonal damage and motor dysfunction. These data suggest that the 5-LO pathway is involved in microglial activation and neuroinflammation and contributes to axonal damage and motor dysfunction.

2. Materials and Methods

2.1. Animal procedures

All animal experiments were performed under a NIH approved animal protocol (NICHD #08-026) approved by the NIH, NICHD Animal Care and Use Committee, in accordance with the NIH guidelines on the care and use of laboratory animals. C57BL/6 male mice (Taconic Farms, Germantown, NY) were received at our facility at 8–10 weeks of age and were fed *ad libitum* a powdered diet (Purina #5002; formulated by Research Diets, New Brunswick, NJ) containing 0.2% cuprizone (bis-cyclohexanone oxaldihydrazone; Sigma, St. Louis, MO). In a preliminary experiment, mice were fed with cuprizone diet for 6 weeks to investigate time-dependent changes of 5-LO gene and protein expression during the demyelination process (Fig. 1A). In the following experiments, mice were fed with cuprizone diet up to 5 weeks, which represents the peak of demyelination, to investigate the effects of 5-LO inhibition on demyelination, neuroinflammation and motor function (Fig. 1D). Mice were maintained on a 12/12h light dark cycle. Mice (n= 7–8 per group) were euthanized with Nembutal and forebrain containing frontal cortex and corpus callosum was dissected on ice. Cerebellum, thalamus, hippocampus, striatum and olfactory bulb were excluded from the dissected samples. Forebrain was rapidly frozen in 2-methylbutane at −50

°C, and stored at −80 °C until use for molecular analysis. For histology, mice (n= 5 per group) were intracardially perfused with 4% paraformaldehyde. Brains were postfixed overnight in 4% paraformaldehyde, subsequently cryoprotected in a 30% sucrose solution, snap frozen and stored at −80 °C until use [31].

2.2. Treatment with MK886

MK886 (Cayman Chemical, Ann Arbor, MI) was dissolved in saline with 5% DMSO, 25% polyethylene glycol-15-hydroxystearate (Solutol, BASF, Ludwigshafen, Germany). MK886 was administered at a dose of 3 mg/kg by intraperitoneal (i.p.) injection once-daily for the last 7 days (week 4 to 5) of cuprizone exposure. Control mice on a normal cuprizone-free diet were treated in parallel with MK886 at the same dose once-daily for 7 days.

2.3. Western blotting

The cytosolic fraction was prepared from forebrain as described [32]. Mice forebrains (n = 6 per group) were homogenized in a homogenizing buffer containing 20 mM Tris-HCl (pH 7.5), using a Polytron® homogenizer. The supernatant was centrifuged at 100,000 × g for 60 min at 4 °C. The supernatant was collected and protein concentration was measured using a Dc Protein Assay kit (Bio-Rad, Richmond, CA). Western blotting was performed as previously described [32]. Briefly, proteins (50 μg) were loaded on Criterion gels (Bio-Rad), transferred onto a polyvinylidene difluoride membrane (Bio-Rad) and immunoblotted with antibodies against 5-LO (1:500; Cayman Chemical) and β-actin (1:3000; Sigma) as loading control. An Odyssey Infrared Imaging System (Licor Biosciences, Lincoln, NB,) was used to detect and quantify protein levels.

2.4. Measurement of IL-6 levels

Forebrains (n = 5 per group) were homogenized in a lysis buffer containing 25 mM Tris-HCl, pH 7.8, 150 mM NaCl, 1 mM EDTA with a complete protease inhibitor cocktail (Roche, Indianapolis, IN). The homogenates were centrifuged at 14,000×g for 20 min, and the supernatant was immediately assayed using a mouse IL-6 ELISA kit (Invitrogen, Carlsbad, CA).

2.5. Histology

Thirty μm-coronal brain sections were cut on a cryostat (Bright Instrument Company, LTD; Huntingdon, England) and mounted on gelatin coated glass slides. Sections were stained with Black Gold II (Histo-Chem, Jefferson, AR) as previously described [33]. Briefly, sections were incubated in a 0.2% Black Gold II solution for 12 min, rinsed in distilled water, fixed in 2% sodium thiosulfate, rinsed in tap water and air-dried. Sections were then cleared in Histo-Clear (National Diagnostics, Atlanta, GA) and coverslipped using DPX (Sigma) mounting medium. Immunohistochemistry was performed using rat anti mouse CD11b (1:200; Serotec, Oxford, UK) as primary antibody at room temperature overnight and visualized using VECTASTAIN ABC kit (Vector Laboratories, Burlingame, CA) and counterstained them with VECTOR hematoxylin QS (Vector). Double immunofluorescence was performed using anti-mouse amyloid precursor protein (APP) (1:200; Chemicon, Temecula, CA) and anti-rabbit neurofilament 200 (NF200) (1:80, Sigma), as follows. Sections were incubated with a mixture of two primary antibodies at room temperature overnight, followed by incubation at room temperature for 1 hour with a mixture of the two secondary antibodies (Alexa Fluor 594 goat anti-mouse IgG and Alexa Fluor 488 goat anti-rabbit IgG (5 μg/ml, Invitrogen). Stained sections were imaged with a Leica TCS SP5confocal microscope system (Leica Microsystems, Wetzlar, Germany). All images were imported into Image J, CD11b positive cells (corpus callosum and cortex) and APP-NF200

double positive axons in the corpus callosum were counted, and densities (counts/mm^2) calculated.

2.6. Quantification of demyelination in the corpus callosum and cortex

Black Gold stained sections were selected between Bregma −0.22 mm and −0.58 mm. Section were photographed (Olympus U-CMAD3 camera) at 10× magnification, the images were opened with Spot Advanced 4.1 software and imported into Image J, which was used to measure the mean optical density within the middle of the corpus callosum, at the level of the fimbria, and of the cortex (primary somatosensory cortex and motor cortex). Optical density in no tissue area was used as blank (backround) and blank was subtracted using Spot Advanced 4.1 software. Myelin densities for each mouse were normalized against optical density values in unchallenged mice using the following formula: myelin score (%) = (density reading/unchallenged density average) × 100.

2.7. RNA extraction and Quantitative Real Time PCR (Q-PCR)

Fresh frozen mouse forebrain (n = 7–8 per group) was processed for RNA extraction using the Qiagen RNeasy Lipid Tissue Mini kit (Qiagen, Valencia, CA) following the manufacturer's procedure. DNase treatment was performed during RNA purification to avoid genomic DNA contamination and RNA purity was verified by examining the 260/280 nm ratio using a spectrophotometer. Extracted RNA was resuspended in RNase free molecular grade water and stored at −80°C until usage. For Q-PCR, total RNA (5 μg) was reverse transcribed using a High Capacity cDNA Archive kit (Applied Biosystems, Foster City, CA).

Q-PCR was performed using the ABI PRISM 7000 Sequence Detection System (Applied Biosystems). Q-PCR results were normalized to phosphoglycerate kinase 1 (PGK1; Mm_00435617_m1) expression levels, as previously reported [32]. Gene expression was analyzed using the following Assays on Demand: Myelin Basic Protein (MBP; Mm01262035_m1); Glial Fibrillary Acidic Protein (GFAP; Mm01253033_m1); Integrin alpha M (CD11b; Mm00434455_m1); Interleukin 6 (IL-6; Mm01210733_m1); Interleukin 1β (IL-1β; Mm99999061_m1); Tumor necrosis factor α (TNFα; Mm00443258_m1); G protein-coupled receptor 17 (GPR17; Mm02619401_s1). Briefly, Taqman Universal PCR Master Mix, Assay-On-Demand primers and cDNA samples were mixed in RNAse-free water and added to an optical 96-well reaction plate (Applied Biosystems). All primers from assay-on-demands (Applied Biosystems) were designed by the company avoiding contaminating genomic DNA amplification by positioning one of the primers over the exon/intron boundary. Negative controls containing no cDNA and a standard curve spanning 3 orders of magnitude of dilution were run on each plate in duplicate. Q-PCR conditions were 50°C for 2 min, 95°C for 10 min, followed by 40 cycles of 15 sec at 95°C and 1 min at 60°C. The amount of target gene expression was calculated by using the $\Delta\Delta C_T$ method [34]. Data were analyzed using relative quantification technique. Relative changes in gene expression were expressed as percent of expression in untreated mice, as previously reported [31].

2.8. Rotarod test

We used an accelerating rotarod treadmill for mice (Mouse rotarod, Ugo Basile, Comerio, Italy) to measure motor balance and coordination. For training, the first day mice (n = 10 per group) were placed on the rod for 5 min at 16, then at 24 and finally at 32 rpm. On the second day, mice were placed on the rod at 16 and 24 rpm (for 5 min, respectively), and allowed to rest for 1 hour. Then mice were tested on the rod at 32 rpm for 5 min. The number of falls from the cylinders were counted and the time each mouse was able to stay

on the rod (latency time) was recorded by a trip switch under the floor of each rotating drum with a maximum recording time of 300 seconds, and computed as the latency to fall [9].

2.9. Statistics

The number of falls from the rotarod was analyzed by a nonparametric Kruscal-Wallis test. All other data were analyzed by one-way ANOVA followed by Newman-Keuls' post hoc test. All data were analyzed using GraphPad Prism Ver. 4.00 (GraphPad Software, Inc., San Diego, CA) and expressed as means ± SEM. p values <0.05 were considered statistically significant.

3. Results

3.1. Gene and protein expression levels of 5-LO

Mice were exposed to cuprizone diet for up to 6 weeks and expression of 5-LO in the forebrain during cuprizone exposure were analyzed. mRNA and protein expression of 5-LO peaked between weeks 4 and 5 (Fig. 1B and C), concomitant to the peak in cuprizone-induced demyelination [6,11].

3.2. Gene expression of glial markers and CD11b immunohistochemistry

To investigate the effects of 5-LO inhibition on neuroinflammation associated with demyelination, we measured gene expression of astrocytic (GFAP) and microglial (CD11b) markers after 5 weeks of cuprizone. mRNA levels of both GFAP and CD11b were increased ($p<0.001$) by cuprizone. While MK886 did not significantly affect cuprizone-induced GFAP upregulation (Fig. 2A), it almost completely inhibited cuprizone-induced increase in CD11b mRNA expression ($p<0.001$; Fig. 2B). We showed by immunostaining that these changes in gene expression were accompanied by changes in protein expression. In normal control mice, microglia immunostaining was only sporadically seen in the corpus callosum and cortex (Fig. 2D and G). Mice exposed to cuprizone showed hypertrophic microglia with enlarged cell bodies and thickened processes (Fig. 2E and H), which were attenuated after MK886 administration (Fig. 2F and I). Cuprizone induced an increase in CD11b-positive cells in the corpus callosum and cortex. The number of CD11b-positive cells was inhibited by MK886 administration in the corpus callosum ($p<0.01$) and cortex ($p<0.001$) (Fig. 2J and K). In MK886-treated mice not exposed to cuprizone, CD11b-positive cells in the corpus callosum and cortex were similar as in control vehicle-treated mice (data not shown).

3.3. Proinflammatory cytokine levels

Cuprizone exposure for 5 weeks increased the mRNA expression of the proinflammatory cytokines IL-1β, TNF-α, and IL-6 ($p<0.001$; Fig. 3). Although the expression level of IL-1β and TNF-α remained unchanged after MK886 treatment, MK886 inhibited cuprizone-induced increase in IL-6 mRNA and protein expression ($p<0.001$; Fig. 3C and D). Treatment with MK886 alone did not change IL-6 protein level (0.095 ± 0.019 pg/mg of tissue) compared to control mice.

3.4. Myelin content

To determine whether the reduction in the neuroinflammatory response to cuprizone by MK886 was accompanied by reduced demyelination, we quantified myelin content in the corpus callosum and cortex with Black Gold staining and measured the mRNA expression of myelin basic protein (MBP). After 5 weeks of cuprizone exposure, we found significant demyelination of the corpus callosum and cortex (Fig. 4A–H), accompanied by a decrease in MBP mRNA expression ($p<0.001$; Fig. 4I). However, treatment with MK886 did not significantly change cuprizone-induced demyelination. MK886-treated control mice not

exposed to cuprizone showed the same level of myelin in the corpus callosum and cortex as control vehicle-treated mice (data not shown).

3.5. Axonal damage and Motor performance

To determine whether a reduction in neuroinflammation by MK886 attenuated cuprizone-induced axonal damage, we performed double immunofluorescence of APP as a marker of axonal damage [35,36] and the axonal marker NF 200 to detect damaged axon (Fig. 5A). Because APP is also expressed in astrocytes [37], we counted APP and NF 200 double positive axons in the corpus callosum. MK886 treatment significantly reduced the number of APP positive axons after 5 weeks of cuprizone ($p<0.05$) (Fig. 5B). Furthermore, GPR17, a newly reported CysLT receptor, has been shown to act as a sensor for neuronal damage [38,39]. Cuprizone exposure induced GPR17 mRNA expression and MK886 treatment attenuated its level ($p<0.05$) (Fig. 5C). Next, we assessed locomotor coordination and balance on a rotarod apparatus. Compared to normal controls, mice exposed to cuprizone recorded a significant decline in locomotion time ($p<0.05$), which was rescued by MK886 treatment (Fig. 5D). MK886 treatment also rescued the cuprizone-induced increase in the number of falls from the rod (Fig. 5E). Overall, MK886 treatment significantly attenuated cuprizone-induced impairment of motor performance.

4. Discussion and conclusions

Using the 5-LO inhibitor MK886 we tested whether 5-LO plays a causative role in the cuprizone-induced demyelinative disease. Although MK886 did not attenuate cuprizone-induced demyelination, it attenuated the increase in IL-6 production and microglial activation. These data suggest that the 5-LO pathway is involved in microglial activation and neuroinflammation independently of the demyelination process. We also demonstrated that inhibition of neuroinflammation by MK886 attenuated axonal damage and motor dysfunction during demyelination, suggesting that 5-LO inhibition may be a useful therapeutic treatment in MS.

IL-6 is known to be involved in neuroinflammatory responses and produced at high level in active MS lesions [40,41]. In our results, MK886 administration inhibited cuprizone-induced IL-6 production and microglial activation, supporting our result, it is reported that LTB_4 induce IL-6 transcription, mRNA expression and protein production [42,43]. In addition, studies of cultured microglia [44], IL-6-deficient mice [45] and IL-6 transgenic mice [46] reveled that IL-6 is important factor in microglial activation. Futhermore, 5-LO pathway may plays a key role in microglial activation directly. Supporting this concept, cultured microglia express cysteinyl-LT receptors (CysLT1 and CysLT2) [47] and inhibition of the 5-LO pathway *in vivo* prevented microglial activation induced by LPS administration or by spreading depression [48,49]. LTB_4 has been shown to upregulate CD11b expression in monocytes [50]. Thus, microglia may also activate CD11b expression *via* LTB_4. Moreover, the suppression of IL-6 production and microglial activation probably result in attenuation of axonal damage and motor dysfunction. Blockade of IL-6 receptor suppressed axonal damage and ameliorated functional recovery after spinal cord injury [51,52]. In MS model, activated microglia is also involved in axonal damage [53] by the mechanism of stripping of synaptic protein [54] and/or microglia-derived glutamate excitotoxicity [55, 56].

Also we demonstrated that MK866 reduced cuprizone-induced expression of GPR17. GPR17, a newly reported Cysteinyl-LT receptor [57], was expressed in microglia/macrophage in the lesioned area of focal ischemia and spinal cord injury [38,39]. It is possible that reduced neuroinflammation would reduce neuronal damage-associated signaling. Taken together, 5-LO inhibition by MK886 leads to suppression of IL-6

production, microglial activation, axonal damage and motor dysfunction by the multi-step mechanism in demyelinating disease.

While it is unclear at this point why MK-886 selectivley decreases cuprizone-induced IL-6, but not IL-1β and TNF-α, we speculate that a possible mechanism involves selective targeting of cytokine producing cells. In a neuroinflammatory situation, microglia produce pro-inflammatory cytokines [58–60] and astrocytes also produce TNFα and IL-1β [61–63]. Thus, in our model, MK886 might inhibit IL-6 production by microglia, but not TNFα and IL-1β by astrocytes.

As previously described [64], we found that cuprizone induced also marked cortical demyelination (Fig. 5). There was no regional difference in the contribution of the 5-LO pathway to demyelination, since MK886 did not affect demyelination levels in either corpus callosum or cortex. A regional accumulation of microglia in the corpus callosum and in the cortical cell layer has been described [65]. Our results indicate that activated microglia is present mainly in the corpus callosum and, to a lesser extent, in the cortex. MK886 treatment attenuated microglial activation and accumulation in both brain areas.

We found that inhibition of the 5-LO pathway did not affect cuprizone-induced demyelination. Similarly, in the EAE model, a 5-LO inhibitor did not significantly reduce clinical score of EAE, even though the onset of EAE was delayed [66]. Furthermore, 5-LO deficient mice developed more severe EAE than wild-type mice [67], although no difference in pathological parameters was detected between deficient mice and control EAE mice with the same clinical score. Thus, both in the EAE and in the cuprizone models of demyelination, the 5-LO pathway does not appear to directly affect myelin levels although its inhibition ameliorates the clinical symptoms of the disease.

Our data demonstrate that the 5-LO pathway plays a key role in microglial activation and neuroinflammation independently of the demyelination process. We also demonstrated that 5-LO inhibition attenuated axonal damage and motor dysfunction during cuprizone-induced demyelination. These results suggest that pharmacological inhibition of 5-LO is a valuable anti-inflammatory treatment for brain inflammation and could provide therapeutic amelioration of MS symptoms.

Acknowledgments

Funding: This work was supported by Intramural Research Program of NIH, National Institute on Aging

This work was supported by Intramural Research Program of NIH, National Institute on Aging. We thank Drs. Sang-Ho Choi and Saba Aid for helpful discussion and technical advice. We thank Dr. Anthony Donsante for kindly providing the rotarod apparatus. We thank Drs. Mukoyama and Onitsuka for kindly providing the confocal microscope and technical advice.

References

1. Kidd D, Barkhof F, McConnell R, Algra PR, Allen IV, Revesz T. Cortical lesions in multiple sclerosis. Brain. 1999; 122(Pt 1):17–26. [PubMed: 10050891]
2. Lucchinetti C, Bruck W, Noseworthy J. Multiple sclerosis: recent developments in neuropathology, pathogenesis, magnetic resonance imaging studies and treatment. Curr Opin Neurol. 2001; 14:259–269. [PubMed: 11371747]
3. Noseworthy JH, Lucchinetti C, Rodriguez M, Weinshenker BG. Multiple sclerosis. N Engl J Med. 2000; 343:938–952. [PubMed: 11006371]
4. Barnett MH, Prineas JW. Relapsing and remitting multiple sclerosis: pathology of the newly forming lesion. Ann Neurol. 2004; 55:458–468. [PubMed: 15048884]

5. Blakemore WF. Demyelination of the superior cerebellar peduncle in the mouse induced by cuprizone. J Neurol Sci. 1973; 20:63–72. [PubMed: 4744511]
6. Matsushima GK, Morell P. The neurotoxicant, cuprizone, as a model to study demyelination and remyelination in the central nervous system. Brain Pathol. 2001; 11:107–116. [PubMed: 11145196]
7. Torkildsen O, Brunborg LA, Myhr KM, Bo L. The cuprizone model for demyelination. Acta Neurol Scand Suppl. 2008; 188:72–76. [PubMed: 18439226]
8. Liu L, Belkadi A, Darnall L, et al. CXCR2-positive neutrophils are essential for cuprizone-induced demyelination: relevance to multiple sclerosis. Nat Neurosci. 2010; 13:319–326. [PubMed: 20154684]
9. Franco-Pons N, Torrente M, Colomina MT, Vilella E. Behavioral deficits in the cuprizone-induced murine model of demyelination/remyelination. Toxicol Lett. 2007; 169:205–213. [PubMed: 17317045]
10. Lucchinetti C, Bruck W, Parisi J, Scheithauer B, Rodriguez M, Lassmann H. Heterogeneity of multiple sclerosis lesions: implications for the pathogenesis of demyelination. Ann Neurol. 2000; 47:707–717. [PubMed: 10852536]
11. Hiremath MM, Saito Y, Knapp GW, Ting JP, Suzuki K, Matsushima GK. Microglial/macrophage accumulation during cuprizone-induced demyelination in C57BL/6 mice. J Neuroimmunol. 1998; 92:38–49. [PubMed: 9916878]
12. Armstrong RC, Le TQ, Flint NC, Vana AC, Zhou YX. Endogenous cell repair of chronic demyelination. J Neuropathol Exp Neurol. 2006; 65:245–256. [PubMed: 16651886]
13. Harbige LS, Sharief MK. Polyunsaturated fatty acids in the pathogenesis and treatment of multiple sclerosis. Br J Nutr. 2007; 98(Suppl 1):S46–553. [PubMed: 17922959]
14. Dworkin RH, Bates D, Millar JH, Paty DW. Linoleic acid and multiple sclerosis: a reanalysis of three double-blind trials. Neurology. 1984; 34:1441–1445. [PubMed: 6387534]
15. Meade CJ, Mertin J, Sheena J, Hunt R. Reduction by linoleic acid of the severity of experimental allergic encephalomyelitis in the guinea pig. J Neurol Sci. 1978; 35:291–308. [PubMed: 632836]
16. Hughes D, Keith AB, Mertin J, Caspary EA. Linoleic acid therapy in severe experimental allergic encephalomyelitis in the guinea-pig: suppression by continuous treatment. Clin Exp Immunol. 1980; 40:523–531. [PubMed: 7418264]
17. Kalyvas A, Baskakis C, Magrioti V, et al. Differing roles for members of the phospholipase A2 superfamily in experimental autoimmune encephalomyelitis. Brain. 2009; 132:1221–1235. [PubMed: 19218359]
18. Marusic S, Leach MW, Pelker JW, et al. Cytosolic phospholipase A2 alpha-deficient mice are resistant to experimental autoimmune encephalomyelitis. J Exp Med. 2005; 202:841–851. [PubMed: 16172261]
19. Whitney LW, Ludwin SK, McFarland HF, Biddison WE. Microarray analysis of gene expression in multiple sclerosis and EAE identifies 5-lipoxygenase as a component of inflammatory lesions. J Neuroimmunol. 2001; 121:40–48. [PubMed: 11730938]
20. Arthur AT, Armati PJ, Bye C, et al. Genes implicated in multiple sclerosis pathogenesis from consilience of genotyping and expression profiles in relapse and remission. BMC Med Genet. 2008; 9:17. [PubMed: 18366677]
21. Neu I, Mallinger J, Wildfeuer A, Mehlber L. Leukotrienes in the cerebrospinal fluid of multiple sclerosis patients. Acta Neurol Scand. 1992; 86:586–587. [PubMed: 1336293]
22. Samuelsson B, Dahlen SE, Lindgren JA, Rouzer CA, Serhan CN. Leukotrienes and lipoxins: structures, biosynthesis, and biological effects. Science. 1987; 237:1171–1176. [PubMed: 2820055]
23. Minami M, Ohno S, Kawasaki H, et al. Molecular cloning of a cDNA coding for human leukotriene A4 hydrolase. Complete primary structure of an enzyme involved in eicosanoid synthesis. J Biol Chem. 1987; 262:13873–13876. [PubMed: 3654641]
24. Haeggstrom JZ, Wetterholm A, Medina JF, Samuelsson B. Leukotriene A4 hydrolase: structural and functional properties of the active center. J Lipid Mediat. 1993; 6:1–13. [PubMed: 8357975]
25. Welsch DJ, Creely DP, Hauser SD, Mathis KJ, Krivi GG, Isakson PC. Molecular cloning and expression of human leukotriene-C4 synthase. Proc Natl Acad Sci U S A. 1994; 91:9745–9749. [PubMed: 7937884]

26. Lam BK, Penrose JF, Freeman GJ, Austen KF. Expression cloning of a cDNA for human leukotriene C4 synthase, an integral membrane protein conjugating reduced glutathione to leukotriene A4. Proc Natl Acad Sci U S A. 1994; 91:7663–7667. [PubMed: 8052639]
27. Vickers PJ. 5-Lipoxygenase-activating protein (FLAP). J Lipid Mediat Cell Signal. 1995; 12:185–194. [PubMed: 8777565]
28. Dixon RA, Diehl RE, Opas E, et al. Requirement of a 5-lipoxygenase-activating protein for leukotriene synthesis. Nature. 1990; 343:282–284. [PubMed: 2300173]
29. Paul L, Fraifeld V, Kaplanski J. Evidence supporting involvement of leukotrienes in LPS-induced hypothermia in mice. Am J Physiol. 1999; 276:R52–58. [PubMed: 9887177]
30. Ciceri P, Rabuffetti M, Monopoli A, Nicosia S. Production of leukotrienes in a model of focal cerebral ischaemia in the rat. Br J Pharmacol. 2001; 133:1323–1329. [PubMed: 11498518]
31. Choi SH, Langenbach R, Bosetti F. Genetic deletion or pharmacological inhibition of cyclooxygenase-1 attenuate lipopolysaccharide-induced inflammatory response and brain injury. FASEB J. 2008; 22:1491–1501. [PubMed: 18162486]
32. Toscano CD, Prabhu VV, Langenbach R, Becker KG, Bosetti F. Differential gene expression patterns in cyclooxygenase-1 and cyclooxygenase-2 deficient mouse brain. Genome Biol. 2007; 8:R14. [PubMed: 17266762]
33. Schmued L, Slikker W Jr. Black-gold: a simple, high-resolution histochemical label for normal and pathological myelin in brain tissue sections. Brain Res. 1999; 837:289–297. [PubMed: 10434014]
34. Livak KJ, Schmittgen TD. Analysis of relative gene expression data using real-time quantitative PCR and the 2(−Delta Delta C(T)) Method. Methods. 2001; 25:402–408. [PubMed: 11846609]
35. Gentleman SM, Nash MJ, Sweeting CJ, Graham DI, Roberts GW. Beta-amyloid precursor protein (beta APP) as a marker for axonal injury after head injury. Neurosci Lett. 1993; 160:139–144. [PubMed: 8247344]
36. Lindner M, Fokuhl J, Linsmeier F, Trebst C, Stangel M. Chronic toxic demyelination in the central nervous system leads to axonal damage despite remyelination. Neurosci Lett. 2009; 453:120–125. [PubMed: 19356606]
37. Clarner T, Buschmann JP, Beyer C, Kipp M. Glial Amyloid Precursor Protein Expression is Restricted to Astrocytes in an Experimental Toxic Model of Multiple Sclerosis. J Mol Neurosci. 2010; 43:268–274. [PubMed: 20607446]
38. Lecca D, Trincavelli ML, Gelosa P, et al. The recently identified P2Y-like receptor GPR17 is a sensor of brain damage and a new target for brain repair. PLoS One. 2008; 3:e3579. [PubMed: 18974869]
39. Ceruti S, Villa G, Genovese T, et al. The P2Y-like receptor GPR17 as a sensor of damage and a new potential target in spinal cord injury. Brain. 2009; 132:2206–2218. [PubMed: 19528093]
40. Cannella B, Raine CS. The adhesion molecule and cytokine profile of multiple sclerosis lesions. Ann Neurol. 1995; 37:424–435. [PubMed: 7536402]
41. Woodroofe MN, Cuzner ML. Cytokine mRNA expression in inflammatory multiple sclerosis lesions: detection by non-radioactive in situ hybridization. Cytokine. 1993; 5:583–538. [PubMed: 8186370]
42. Rola-Pleszczynski M, Stankova J. Leukotriene B4 enhances interleukin-6 (IL-6) production and IL-6 messenger RNA accumulation in human monocytes in vitro: transcriptional and posttranscriptional mechanisms. Blood. 1992; 80:1004–1011. [PubMed: 1323342]
43. Stankova J, Rola-Pleszczynski M. Interleukin 6 production by mononuclear phagocytes can be stimulated by leukotrienes. Arch Immunol Ther Exp (Warsz). 1992; 40:17–21. [PubMed: 1336653]
44. Streit WJ, Hurley SD, McGraw TS, Semple-Rowland SL. Comparative evaluation of cytokine profiles and reactive gliosis supports a critical role for interleukin-6 in neuron-glia signaling during regeneration. J Neurosci Res. 2000; 61:10–20. [PubMed: 10861795]
45. Klein MA, Moller JC, Jones LL, Bluethmann H, Kreutzberg GW, Raivich G. Impaired neuroglial activation in interleukin-6 deficient mice. Glia. 1997; 19:227–233. [PubMed: 9063729]
46. Fattori E, Lazzaro D, Musiani P, Modesti A, Alonzi T, Ciliberto G. IL-6 expression in neurons of transgenic mice causes reactive astrocytosis and increase in ramified microglial cells but no neuronal damage. Eur J Neurosci. 1995; 7:2441–2449. [PubMed: 8845949]

47. Ballerini P, Di Iorio P, Ciccarelli R, et al. P2Y1 and cysteinyl leukotriene receptors mediate purine and cysteinyl leukotriene co-release in primary cultures of rat microglia. Int J Immunopathol Pharmacol. 2005; 18:255–268. [PubMed: 15888248]
48. Caggiano AO, Kraig RP. Eicosanoids and nitric oxide influence induction of reactive gliosis from spreading depression in microglia but not astrocytes. J Comp Neurol. 1996; 369:93–108. [PubMed: 8723705]
49. Willard LB, Hauss-Wegrzyniak B, Danysz W, Wenk GL. The cytotoxicity of chronic neuroinflammation upon basal forebrain cholinergic neurons of rats can be attenuated by glutamatergic antagonism or cyclooxygenase-2 inhibition. Exp Brain Res. 2000; 134:58–65. [PubMed: 11026726]
50. Vaddi K, Newton RC. Regulation of monocyte integrin expression by beta-family chemokines. J Immunol. 1994; 153:4721–4732. [PubMed: 7525713]
51. Mukaino M, Nakamura M, Yamada O, et al. Anti-IL-6-receptor antibody promotes repair of spinal cord injury by inducing microglia-dominant inflammation. Exp Neurol. 2010; 224:403–414. [PubMed: 20478301]
52. Okada S, Nakamura M, Mikami Y, et al. Blockade of interleukin-6 receptor suppresses reactive astrogliosis and ameliorates functional recovery in experimental spinal cord injury. J Neurosci Res. 2004; 76:265–276. [PubMed: 15048924]
53. Howell OW, Rundle JL, Garg A, Komada M, Brophy PJ, Reynolds R. Activated microglia mediate axoglial disruption that contributes to axonal injury in multiple sclerosis. J Neuropathol Exp Neurol. 2010; 69:1017–1033. [PubMed: 20838243]
54. Rasmussen S, Wang Y, Kivisakk P, et al. Persistent activation of microglia is associated with neuronal dysfunction of callosal projecting pathways and multiple sclerosis-like lesions in relapsing--remitting experimental autoimmune encephalomyelitis. Brain. 2007; 130:2816–2829. [PubMed: 17890734]
55. Pitt D, Werner P, Raine CS. Glutamate excitotoxicity in a model of multiple sclerosis. Nat Med. 2000; 6:67–70. [PubMed: 10613826]
56. Fu Y, Sun W, Shi Y, Shi R, Cheng JX. Glutamate excitotoxicity inflicts paranodal myelin splitting and retraction. PLoS One. 2009; 4:e6705. [PubMed: 19693274]
57. Ciana P, Fumagalli M, Trincavelli ML, et al. The orphan receptor GPR17 identified as a new dual uracil nucleotides/cysteinyl-leukotrienes receptor. EMBO J. 2006; 25:4615–4627. [PubMed: 16990797]
58. Banati RB, Gehrmann J, Schubert P, Kreutzberg GW. Cytotoxicity of microglia. Glia. 1993; 7:111–118. [PubMed: 8423058]
59. Giulian D, Corpuz M. Microglial secretion products and their impact on the nervous system. Adv Neurol. 1993; 59:315–320. [PubMed: 8420117]
60. McGeer PL, McGeer EG. The inflammatory response system of brain: implications for therapy of Alzheimer and other neurodegenerative diseases. Brain Res Brain Res Rev. 1995; 21:195–218. [PubMed: 8866675]
61. Lau LT, Yu AC. Astrocytes produce and release interleukin-1, interleukin-6, tumor necrosis factor alpha and interferon-gamma following traumatic and metabolic injury. J Neurotrauma. 2001; 18:351–359. [PubMed: 11284554]
62. Corsini E, Dufour A, Ciusani E, et al. Human brain endothelial cells and astrocytes produce IL-1 beta but not IL-10. Scand J Immunol. 1996; 44:506–511. [PubMed: 8947603]
63. Sawada M, Kondo N, Suzumura A, Marunouchi T. Production of tumor necrosis factor-alpha by microglia and astrocytes in culture. Brain Res. 1989; 491:394–397. [PubMed: 2765895]
64. Skripuletz T, Lindner M, Kotsiari A, et al. Cortical demyelination is prominent in the murine cuprizone model and is strain-dependent. Am J Pathol. 2008; 172:1053–1061. [PubMed: 18349131]
65. Gudi V, Moharregh-Khiabani D, Skripuletz T, et al. Regional differences between grey and white matter in cuprizone induced demyelination. Brain Res. 2009; 1283:127–138. [PubMed: 19524552]
66. Marusic S, Thakker P, Pelker JW, et al. Blockade of cytosolic phospholipase A2 alpha prevents experimental autoimmune encephalomyelitis and diminishes development of Th1 and Th17 responses. J Neuroimmunol. 2008; 204:29–37. [PubMed: 18829119]

67. Emerson MR, LeVine SM. Experimental allergic encephalomyelitis is exacerbated in mice deficient for 12/15-lipoxygenase or 5-lipoxygenase. Brain Res. 2004; 1021:140–145. [PubMed: 15328042]

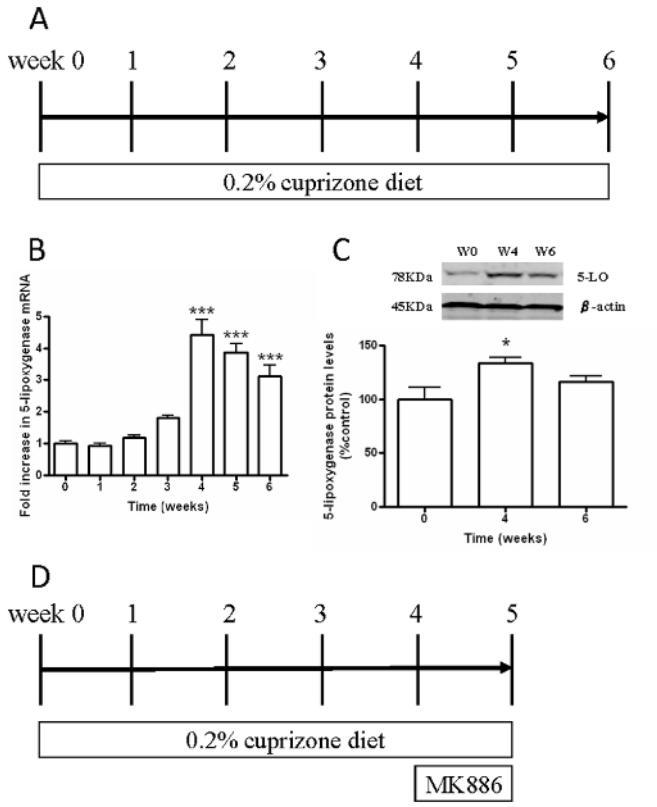

Figure 1. Study design and 5-LO expression levels

In a preliminary experiment, mice were fed with the cuprizone diet for 6 weeks to investigate 5-LO expression levels (A). Gene expression of 5-LO relative to pgk-1, as determined by real-time PCR (B) and protein levels as determined by western blotting (C) in the forebrain of cuprizone-exposed up to 6 weeks and control mice. Data are means ± SEM, n = 6, respectively. Statistical analysis was performed using one-way ANOVA followed by post-hoc Newman-Keuls test (*p<0.05, ***p<0.001 vs. week 0). In the following experiments, mice were fed with cuprizone diet up to 5 weeks and injected with MK886 i.p. once-daily for the last 7 days (week 4 to 5) of cuprizone exposure (D).

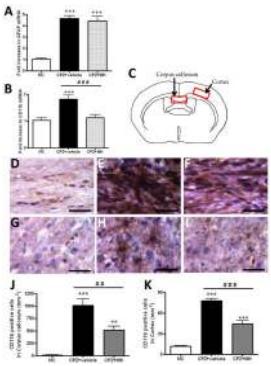

Figure 2. Relative gene expression of glial markers and CD11b immunostaining

Gene expression of GFAP (A) and CD11b (B) relative to pgk-1, as determined by real-time PCR in the forebrain after 5 weeks of cuprizone exposure. Data are means ± SEM, n = 7–8. Statistical analysis was performed using one-way ANOVA followed by post-hoc Newman-Keuls test (***p<0.001 vs. normal controls: ###p<0.001 vs. CPZ+vehicle). Schematic diagram of the mouse brain in coronal section. The red line marks the area of corpus callosum and cortex analyzed for CD11b positive cells after 5 weeks of cuprizone (C). Immunostaining with anti-CD11b (D–I) showed microglial activation. Coronal brain sections of corpus callosum (D: normal control, E: CPZ, F: CPZ+MK886) and cortex (G: normal control, H: CPZ, I: CPZ+MK886). Scale bars = 50 μm. Number of microglia in the corpus callosum (J) and cortex (K). Data are means ± SEM, n = 5, respectively. Statistical analysis was performed using one-way ANOVA followed by post-hoc Newman-Keuls test (**p<0.01, ***p<0.001 vs. normal controls: ###p<0.001, ##p<0.01 vs. CPZ+vehicle).

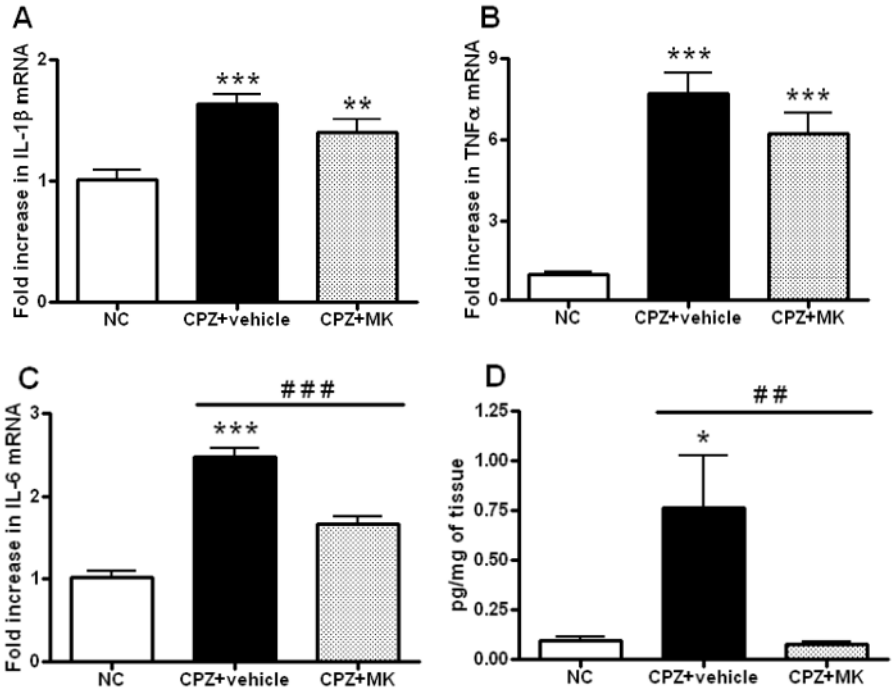

Figure 3. Pro-inflammatory cytokine levels

Gene expression of IL-1β (A), TNF-α (B) and IL-6 (C) relative to pgk-1, as determined by real-time PCR in the forebrain after 5 weeks of cuprizone. Data are means ± SEM, n = 7–8. Statistical analysis was performed using one-way ANOVA followed by post-hoc Newman-Keuls test (**p<0.01, ***p<0.01 vs. normal controls: ###p<0.001 vs. CPZ+vehicle). IL-6 protein levels (D) in the forebrain. Data are means ± SEM, n = 5. Statistical analysis was performed using one-way ANOVA followed by post-hoc Newman-Keuls test (*p<0.05 vs. normal controls: ##p<0.01 vs. CPZ+vehicle).

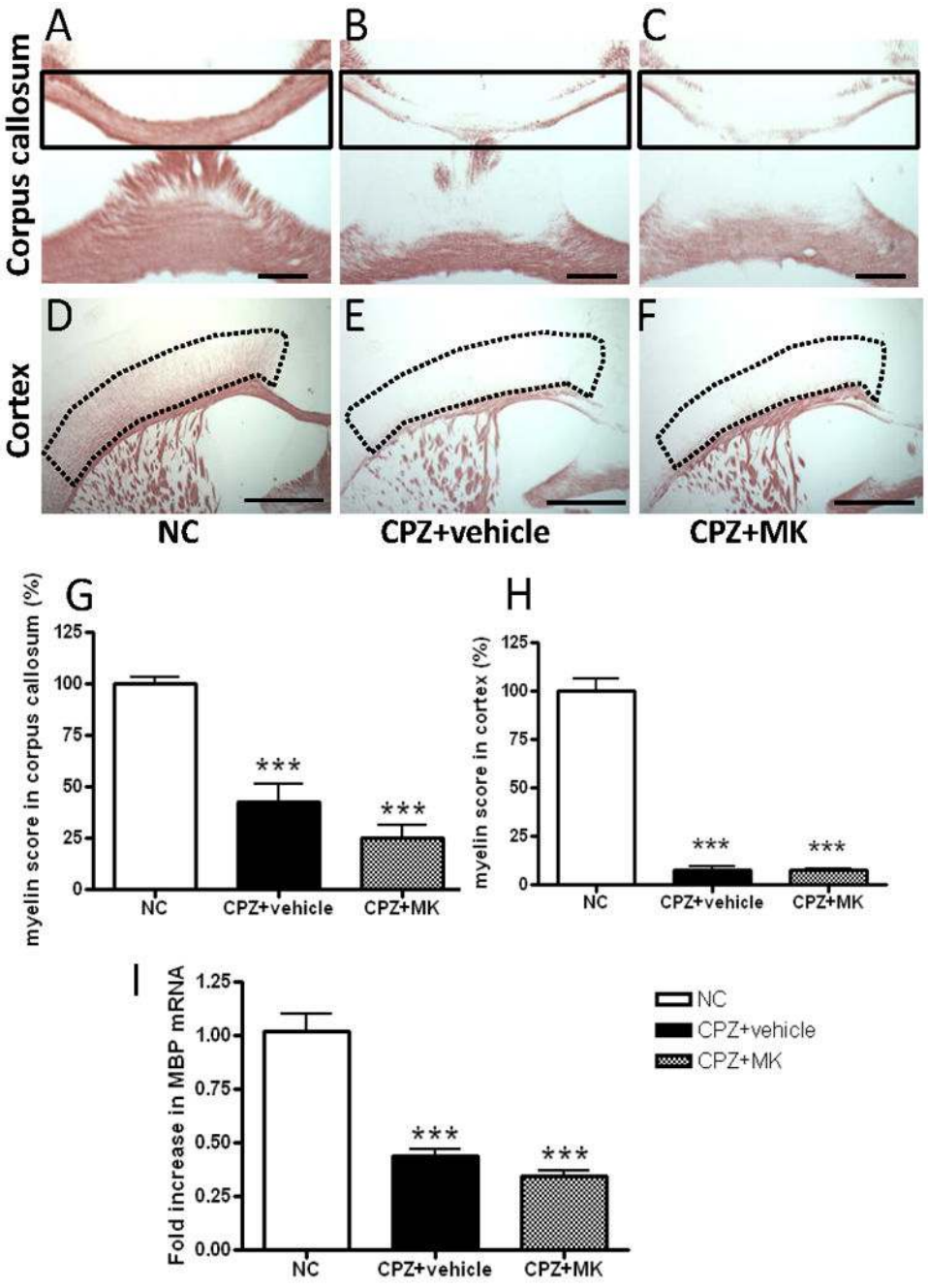

Figure 4. Black Gold staining of myelin and MBP gene expression

Representative photomicrographs of coronal brain sections at the level of the fimbria demonstrate a progressive demyelination of the corpus callosum (A–C) and cortex (D–F) after 5 weeks of cuprizone treatment. Black gold staining of normal control (A and D), CPZ +vehicle (B and E) and CPZ + MK886 (C and F). Myelin densities of the corpus callosum (G) and cortex (H) were compared with normal controls and expressed as a percentage of control values using the Image J analysis program (***$p<0.001$ vs. normal controls). Gene expression of MBP (I) relative to pgk-1, as determined by real-time PCR in the forebrain. Data are mean ± SEM, n = 7–8. Statistical analysis was performed using one-way ANOVA

followed by post-hoc Newman-Keuls test (***p<0.001 vs. normal controls). Scale bar for (A–C) = 500 μm. Scale bar for (D–F) = 1 mm.

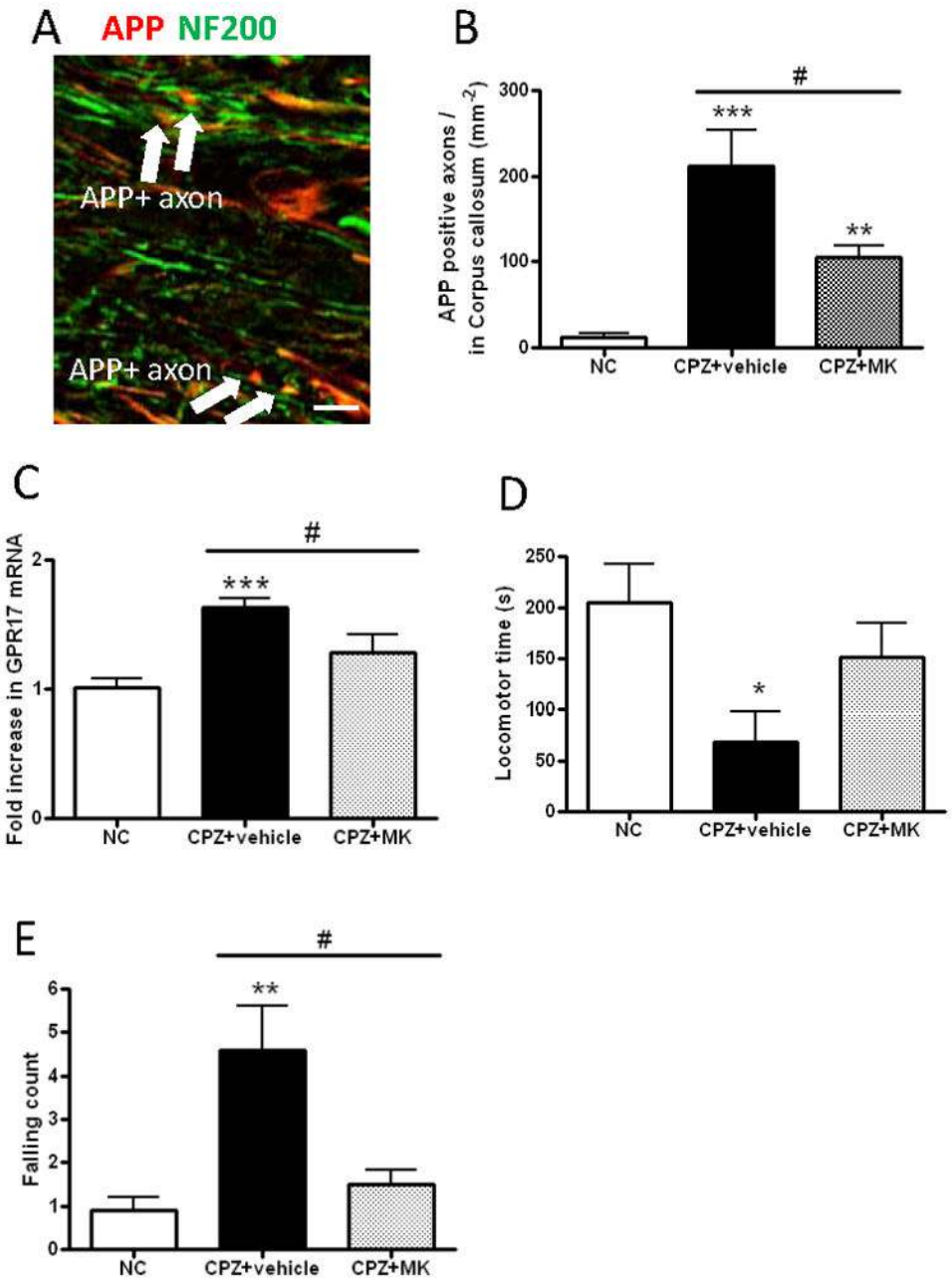

Figure 5. MK886 treatment attenuates cuprizone-induced axonal damage and motor deficits

Representative sections show APP and NF200 double positive axon in the corpus callosum (A) after 5 weeks of cuprizone. Scale bars = 10 μm. Number of APP and NF200 double positive axon in the corpus callosum (B). Data are means ± SEM, n = 5, respectively. Statistical analysis was performed using one-way ANOVA followed by post-hoc Newman-Keuls test (**p<0.01, ***p<0.001 vs. normal controls: #p<0.05 vs. CPZ+vehicle). Gene expression of GPR17 relative to pgk-1, as determined by real-time PCR in the forebrain after 5 weeks of cuprizone (C). Data are expressed as mean ± SEM., n = 7–8. Statistical analysis was performed using one-way ANOVA followed by post-hoc Newman-Keuls test (***p<0.001 vs. normal controls: #p<0.05 vs. CPZ+vehicle). Mice were assessed for locomotion time for 300 sec (D). Data are means ± SEM, n = 10 per group. Statistical

analysis was performed using one-way ANOVA followed by post-hoc Newman-Keuls test (*p<0.05 vs. normal controls). Number of falls on the rotarod test (E). Data are mean ± SEM., n = 10 per group. Statistical analysis was performed using nonparametric Kruscal-Wallis test (*p<0.05, **p<0.01 vs. normal controls: #p<0.05 vs. CPZ+vehicle).